

Substituent Effects on Exchange Coupling: 5-Aryl-Substituted Semiquinones and Their Complexes with Mn^{II} and Cu^{II}

David A. Shultz,^{*,†} Joseph C. Sloop,^{*,‡} Tashni-Ann Coote,[†] Mithra Beikmohammadi,[#] Jeff Kampf,[§] and Paul D. Boyle[†]

Department of Chemistry, North Carolina State University, P.O. Box 8204, Raleigh, North Carolina 27695, Department of Chemistry and Life Science, United States Military Academy, 646 Swift Road, West Point, New York 10996, and Department of Chemistry, University of Michigan, Ann Arbor, Michigan 48109-1055

Received September 22, 2006

A series of functionalized radical anion semiquinone (SQ-Ar) ligands and their Mn^{II}- and Cu^{II}-hydro-tris(3-cumenyl-5-methylpyrazolyl)borate (Tp^{Cum,Me}M^{II}) complexes were prepared and characterized. The semiquinone ligands have substituted phenyl rings (Ar = -C₆H₅NO₂, -C₆H₅OMe, -C₆H₅-*tert*-Bu, etc.) attached to the SQ 5-position. Despite the “remoteness” of the phenyl ring substituents, the M^{II}-SQ exchange parameters, *J*, were found to vary nearly 3-fold. Attempts to quantify the substituent effects on *J* are complicated by the fact that not all complexes could be structurally characterized. As such, substituent effects and phenyl-ring torsion angles could conspire to produce the observed variation in *J* values. Although there is no clear trend in the *J* values as a function of SQ substituent for the Mn^{II} complexes, for the Cu^{II} complexes, electron-withdrawing substituents on the phenyl ring have greater ferromagnetic *J* values than the Cu^{II} complexes of SQ ligands with electron-donating substituents. This trend suggests a FM contribution from MLCT excited states in the copper complexes.

Introduction

Control of electron spin–spin exchange coupling offers exciting challenges in molecular structure–property relationships that could help shape the future of molecule-based electronic^{1–4} and spintronic materials.^{5–8} In accordance with the Goodenough–Kanamoori rules, the classic work of

Hatfield and co-workers and the corresponding theory of Hoffman showed how molecular geometry affected both the sign and magnitude of exchange coupling in bridged binuclear metal complexes.^{9–11} In the organic realm, previous research has shown that π -connectivity is critical in determining the sign of the exchange parameter in exchange-coupled organic biradicals,^{12–14} while our group^{15,16} and others^{17,18} have shown that molecular conformation, electron

* To whom correspondence should be addressed. E-mail: David_Shultz@ncsu.edu (D.A.S.); Joseph.Sloop@usma.edu (J.C.S.).

[†] North Carolina State University.

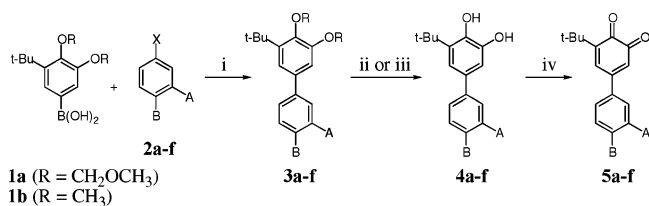
[‡] United States Military Academy.

[§] University of Michigan.

[#] NCSU Undergraduate Researcher, 1999–2001.

- (1) Beni, A.; Dei, A.; Shultz, D. A.; Sorace, L. *Chem. Phys. Lett.* **2006**, *428*, 400–404.
- (2) Dei, A.; Gatteschi, D.; Sangregorio, C.; Sorace, L. *Acc. Chem. Res.* **2004**, *37*, 827–835.
- (3) Picraux, L. B.; Smeigh, A. L.; Guo, D.; McCusker, J. K. *Inorg. Chem.* **2005**, *44*, 7846–7865.
- (4) Rodriguez, J. H.; Wheeler, D. E.; McCusker, J. K. *J. Am. Chem. Soc.* **1998**, *120*, 12051–12068.
- (5) Tagami, K.; Tsukada, M. *J. Phys. Chem. B* **2004**, *108*, 6441–6444.
- (6) Liang, W.; Shores, M. P.; Bockrath, M.; Long, J. R.; Park, H. *Nature* **2002**, *417*, 725–729.
- (7) Tiba, M. V.; Kurnosikov, O.; Flipse, C. F. J.; Koopmans, B.; Swagten, H. J. M.; Kohlhepp, J. T.; de Jonge, W. J. M. *Surf. Sci.* **2002**, *498*, 161–167.
- (8) Wolf, S. A.; Awschalom, D. D.; Buhrman, R. A.; Daughton, J. M.; von Molnar, S.; Roukes, M. L.; Chtchelkanova, A. Y.; Treger, D. M. *Science* **2001**, *294*, 1488–1495.

- (9) Hatfield, W. E. Properties of Condensed Compounds (Compounds with Spin Exchange). In *Theory and Applications of Molecular Paramagnetism*; Boudreaux, E. A., Mulay, L. N., Ed.; Wiley-Interscience: New York, 1976; Chapter 7, pp 381–385.
- (10) Crawford, V. H.; Richardson, H. W.; Wasson, J. R.; Hodgson, D. J.; Hatfield, W. E. *Inorg. Chem.* **1976**, *15*, 2107–2110.
- (11) Hay, P. J.; Thibeault, J. C.; Hoffmann, R. *J. Am. Chem. Soc.* **1975**, *97*, 4884–4899.
- (12) Dougherty, D. A. *Acc. Chem. Res.* **1991**, *24*, 88–94.
- (13) Lahti, P. M. *Magnetic Properties of Organic Materials*; Marcel Dekker: New York, 1999.
- (14) Rajca, A. *Chem. Rev.* **1994**, *94*, 871–893.
- (15) Shultz, D. A.; Fico, R. M. Jr.; Lee, H.; Kampf, J. W.; Kirschbaum, K.; Pinkerton, A. A.; Boyle, P. D. *J. Am. Chem. Soc.* **2003**, *125*, 15426–15432.
- (16) Shultz, D. A.; Fico, R. M., Jr.; Bodnar, S. H.; Kumar, R. K.; Vostrikova, K. E.; Kampf, J. W.; Boyle, P. D. *J. Am. Chem. Soc.* **2003**, *125*, 11761–11771.
- (17) Rajca, A.; Utamapanya, S.; Smithhisler, D. J. *J. Org. Chem.* **1993**, *58*, 5650–5652.

Scheme 1^a

^a Conditions: (i) 5 mol % Pd(PPh₃)₄, C₂H₅OH (1–10 mL), 2 M Na₂CO₃ (1–15 mL), THF (20–50 mL), reflux (20–30h); (ii) (R = CH₂OCH₃) CH₃OH (50–70 mL), HCl (2 mL), reflux (18 h); (iii) (R = CH₃) BBr₃ (3 equiv), CH₂Cl₂ (10 mL), –78 °C → room temp, 20 h; (iv) Fétizon's Reagent (3–5 g), Na₂SO₄ (3–5 g), CH₂Cl₂ (20 mL), 18 h, room temp.

delocalization^{19,20} and substituent effects^{21–23} can modulate the exchange parameter, *J*, in organic systems.

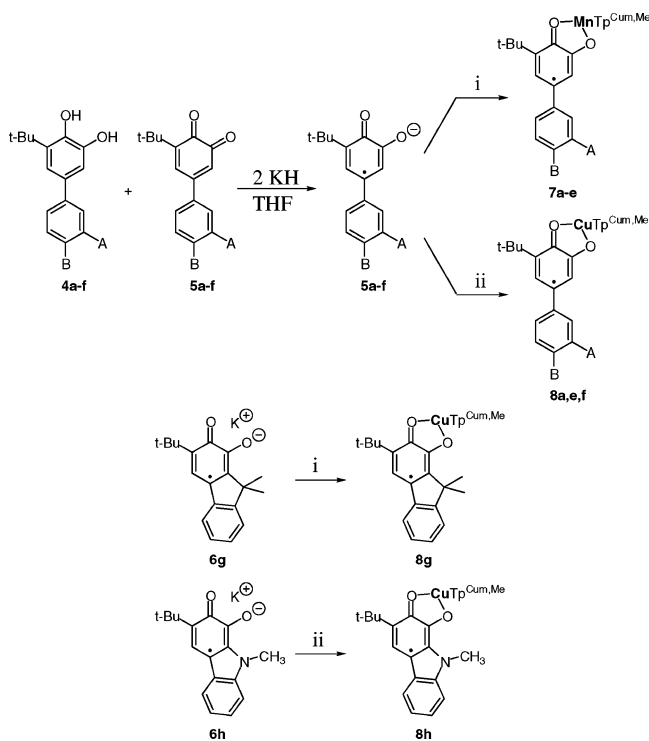
One of the most exciting classes of exchange-coupled systems are the paramagnetic ligand–paramagnetic metal ion species.^{24,25} In these fascinating complexes, both direct- and superexchange mechanisms can make strong contributions to the exchange parameter, and therefore several opportunities exist for studying substituent effects on exchange coupling. Along these lines, we prepared several functionalized semiquinone (SQ-Ar) ligands and their 5-coordinate Mn^{II}- and Cu^{II}hydro-tris(3-cumenyl-5-methylpyrazolyl)borate complexes, Tp^{Cum,Me}Mn^{II}(SQ-Ar) and Tp^{Cum,Me}Cu^{II}(SQ-Ar).

These two classes of metal complexes were chosen to provide examples of substituent effects on exchange coupling for both antiferromagnetic metal–ligand exchange (Mn^{II}SQ-Ar)^{25,26} and ferromagnetic exchange (Cu^{II}SQ-Ar).^{25–27} The SQ-Ar ligands exhibit a “remote” substituent effect in that the substituents themselves are bound to a phenyl ring attached to the 5-position of the SQ ligand. We chose this substituent pattern to avoid the formation of other charge distributions that might arise from strong electron-withdrawing groups, NO₂ for example.^{28,29}

Results and Discussion

Ligand and Metal Complex Synthesis. Scheme 1 depicts our synthetic approach and the yields for the SQ-Ar

- (18) Silverman, S. K.; Dougherty, D. A. *J. Phys. Chem.* **1993**, *97*, 13273–13283.
 (19) Shultz, D. A.; Kumar, R. K. *J. Am. Chem. Soc.* **2001**, *123*, 6431–6432.
 (20) Franzen, S.; Shultz, D. A. *J. Phys. Chem. A* **2003**, *107*, 4292–4299.
 (21) Shultz, D. A.; Bodnar, S. H.; Lee, H.; Kampf, J. W.; Incarvito, C. D.; Rheingold, A. L. *J. Am. Chem. Soc.* **2002**, *124*, 10054–10061.
 (22) West, A. P., Jr.; Silverman, S. K.; Dougherty, D. A. *J. Am. Chem. Soc.* **1996**, *118*, 1452–1463.
 (23) Borden, W. T. Qualitative and Quantitative Predictions and Measurements of Singlet-Triplet Splittings in Non-Kekule Hydrocarbon Diradicals and Heteroatom Derivatives. In *Magnetic Properties of Organic Materials*; Lahti, P. M., Ed.; Marcel Dekker: New York, 1999; Chapter 5.
 (24) Caneschi, A.; Gatteschi, D.; Sessoli, R.; Rey, P. *Acc. Chem. Res.* **1989**, *22*, 392–398.
 (25) Dei, A.; Gatteschi, D. *Inorg. Chim. Acta.* **1992**, *198–200*, 813–822.
 (26) Shultz, D. A.; Vostrikova, K. E.; Bodnar, S. H.; Koo, H. J.; Whangbo, M. H.; Kirk, M. L.; Depperman, E. C.; Kampf, J. W. *J. Am. Chem. Soc.* **2003**, *125*, 1607–1617.
 (27) Ruf, M.; Noll, B. C.; Groner, M. D.; Yee, G. T.; Pierpont, C. G. *Inorg. Chem.* **1997**, *36*, 4860–4865.
 (28) Ruf, M.; Lawrence, A. M.; Noll, B. C.; Pierpont, C. G. *Inorg. Chem.* **1998**, *37*, 1992–1999.
 (29) Shultz, D. A.; Bodnar, S. H.; Kumar, R. K.; Lee, H.; Kampf, J. W. *Inorg. Chem.* **2001**, *40*, 546–549.

Scheme 2^a

^a Conditions: (i) (1) Mn(ClO₄)₂·6H₂O (1 equiv, ~0.15 mmol), KTp^{Cum,Me} (1 equiv, ~0.15 mmol), THF (~5 mL), 1 h, (2) SQ (1 equiv), 1 h; (ii) (1) Cu(ClO₄)₂·6H₂O (1 equiv, ~0.15 mmol), KTp^{Cum,Me} (1 equiv, ~0.15 mmol), THF (~5 mL), 1 h, (2) SQ (1 equiv), 1 h.

precursors, which were characterized in the usual fashion.^{30–32} Synthetic yields are presented in Table S1 (see Supporting Information). One note of interest is our use of a one-pot Suzuki coupling reaction,³³ which in most cases, led to improved biaryl product yields.

With the catechols and quinones in hand, a simple comproportionation reaction carried out under air-free conditions provided the target SQ-Ar ligands, **6a–6f**, as well as two planar SQ-Ar ligands, **6g** and **6h**.³⁴ These were subsequently reacted with (Tp^{Cum,Me}Mn^{II})⁺ and (Tp^{Cum,Me}Cu^{II})⁺ yielding compounds **7a–7e** and **8a**, **8e**, **8f**, **8g**, and **8h** respectively (Scheme 2). Yields are listed in Table S2 (see Supporting Information) only for those complexes that could be isolated in pure form.

Recrystallization of both the Tp^{Cum,Me}Mn^{II}(SQ-Ar) and Tp^{Cum,Me}Cu^{II}(SQ-Ar) complexes to obtain X-ray crystallographic structures posed challenges, often requiring solvent mixtures. In one case, **7e**, a pyrazole moiety was found to add to the semiquinone ring, but it is unknown if this occurred during complex formation, or if it formed during complex decomposition. This type of addition is known to

- (30) Shultz, D. A.; Boal, A. K.; Driscoll, D. J.; Kitchin, J. R.; Tew, G. N. *J. Org. Chem.* **1995**, *60*, 3578.
 (31) Shultz, D. A.; Boal, A. K.; Lee, H.; Farmer, G. T. *J. Org. Chem.* **1998**, *63*, 9462–9469.
 (32) Shultz, D. A.; Boal, A. K.; Driscoll, D. J.; Farmer, G. T.; Hollomon, M. G.; Kitchin, J. R.; Miller, D. B.; Tew, G. N. *Mol. Cryst. Liq. Cryst.* **1997**, *305*, 303–310.
 (33) Baudoin, O.; Guenard, D.; Gueritte, F. *J. Org. Chem.* **2000**, *65*, 9268–9271.
 (34) Shultz, D. A.; Sloop, J. C.; Washington, Gary *J. Org. Chem.* **2006**, *71*, published online October 20, <http://dx.doi.org/10.1021/jo061502j>.

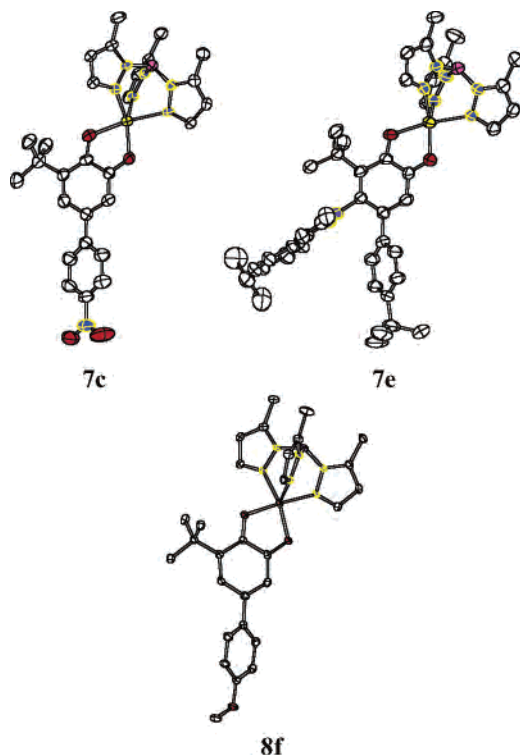


Figure 1. ORTEP representations of the crystal structures of **7c**, **7e**, and **8f**. The thermal ellipsoids are drawn at the 50% probability level. The hydrogens and cumenyl groups are excluded for clarity.

occur in other complexes, a methoxy group added to a complex in the same position.²⁶ Nevertheless, X-ray quality crystals were obtained for two $\text{Tp}^{\text{Cum,Me}}\text{Mn}(\text{SQ-Ar})$ complexes, **7c** and **7e**, and one $\text{Tp}^{\text{Cum,Me}}\text{Mn}(\text{SQ-Ar})$ complex, **8f**. The ORTEP diagrams for complexes **7c**, **7e**, and **8f** are shown in Figure 1, and the key crystal data are reported in Table 1.

The bond lengths listed in Supporting Information (Tables S3–5) are very close to the “typical” semiquinone values.³⁵

The aryl ring/semiquinone ring torsion angles found in complexes **7c**, **7e**, and **8f**, which range from 23 to 43°, are of interest in determining whether there is attenuation in the ability of a substituent by mesomeric interaction to modulate J . However, without a more complete series of crystallographic data, it is difficult to relate ring torsion angles to effectiveness of the substituent to modulate molecular properties. In addition, complex **7e** has a cumenyl-methylpyrazole group attached to the SQ ring. The pyrazole group is an unwanted second substituent that further complicates the analysis of substituent effects on exchange coupling.

Variable-Temperature Magnetic Susceptibility. As shown in Figure 2 for the $\text{Mn}^{\text{II}}(\text{SQ})\text{Tp}^{\text{Cum,Me}}$ complexes, the high-temperature value of the molar paramagnetic susceptibility-temperature product, χT , is considerably less than the theoretical value ($\chi T(\text{Mn}^{\text{II}}) + \chi T(\text{SQ-Ar}) = 4.75 \text{ emu K mol}^{-1}$), consistent with a net antiferromagnetic interaction between Mn^{II} and SQ-Ar.²⁶ Indeed, as 2 K is approached, the χT values tend toward $\sim 3 \text{ emu K mol}^{-1}$, the expected value for a ground quintet state.

In stark contrast to the Mn^{II} complexes, the $\text{Tp}^{\text{Cum,Me}}\text{Cu}^{\text{II}}(\text{SQ-Ar})$ complexes exhibit χT values near room-temperature which are considerably greater than the sum of metal and ligand spins ($0.75 \text{ emu K mol}^{-1}$), consistent with the expected ferromagnetic coupling (Figure 3).^{27,36} As expected, as the temperature is lowered, the χT values tend toward 1 emu K mol^{-1} , where population of the ground triplet state approaches 100%.

The decrease of the χT data at very low temperatures (below 5 K) for both series of complexes was observed and accounted for with a mean field correction (ϑ), using the expression $\chi_{\text{eff}} = \chi/(1 - \vartheta\chi)$, where $\vartheta = 2zJ'/(Ng^2\beta^2)$,^{37,38} zJ' measures (weak) intermolecular interactions, and N , g , and β have their usual meaning. The χT versus temperature plots for both the $\text{Tp}^{\text{Cum,Me}}\text{Mn}^{\text{II}}(\text{SQ-Ar})$ and $\text{Tp}^{\text{Cum,Me}}\text{Cu}^{\text{II}}(\text{SQ-Ar})$ complexes were fit using the $\chi T(T)$ expressions for the Mn^{II} (eq 1) and Cu^{II} complexes (eq 2). Equations 1 and 2

$$\chi T = \frac{Ng^2\beta^2}{3k} \frac{30 + 84e^{-6J/kT}}{5 + 7e^{-6J/kT}} \quad (1)$$

$$\chi T = \frac{Ng^2\beta^2}{3k} \frac{6}{3 + e^{-2J/kT}} \quad (2)$$

were derived using the spin Hamiltonian $H = -2J\hat{S}_1\hat{S}_2$, where J is the metal-SQ-Ar spin-spin exchange coupling parameter and \hat{S}_1 and \hat{S}_2 are metal and SQ-Ar spins, respectively. Fit parameters for the χT versus T plots are reported in Table 2.

For both the $\text{Tp}^{\text{Cum,Me}}\text{Mn}^{\text{II}}$ - and $\text{Tp}^{\text{Cum,Me}}\text{Cu}^{\text{II}}(\text{SQ-Ar})$ complexes, there is an approximate 2- to 3-fold variation in the magnitude of J . The $\text{Tp}^{\text{Cum,Me}}\text{Mn}^{\text{II}}(\text{SQ-Ar})$ complex J values are rather scattered, likely resulting from the five exchange pathways possible between the $d^5 \text{Mn}^{\text{II}}$ species and the $S = 1/2$ semiquinone ligand. For each substituent, one exchange pathway may predominate over the other available pathways, resulting in variation of the J values.

However, in the $\text{Tp}^{\text{Cum,Me}}\text{Cu}^{\text{II}}(\text{SQ-Ar})$ complexes, it appears that electron-withdrawing groups increase the magnitude of ferromagnetic J relative to that of electron donors. Since electron-withdrawing substituents will lower the energy of ligand π^* levels, this observation suggests that MLCT states make important ferromagnetic contributions to J . We must note however that since we do not have crystal structures for all of these complexes, we cannot deconvolute substituent effects from conformation effects (differences in Ar-ring torsion angles). Large Ar-ring torsion angles will modulate the electron-donating and -withdrawing ability of the substituents. However, in two cases (**8g** and **8h**), the ligand conformation is irrelevant since the Ar ring is fused to the SQ ring. In these two cases, there appears to be little difference between the strongly donating N -methyl nitrogen of the carbazole and the more weakly donating $\text{C}(\text{Me})_2$ of the fluorenyl group, suggesting the need for further study.

(36) Benelli, C.; Dei, A.; Gatteschi, D.; Pardi, L. *Inorg. Chem.* **1990**, *29*, 3409–3415.

(37) O'Connor, C. J. *Prog. Inorg. Chem.* **1982**, *29*, 203–283.

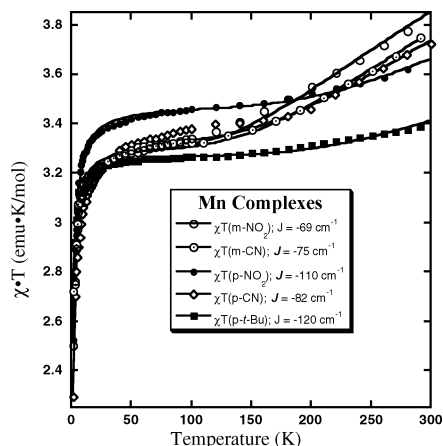
(38) Caneschi, A.; Dei, A.; Lee, H.; Shultz, D. A.; Sorace, L. *Inorg. Chem.* **2001**, *40*, 408–411.

(35) Shultz, D. A.; Bodnar, S. H.; Kampf, J. W. *Chem. Commun.* **2001**, 93–94.

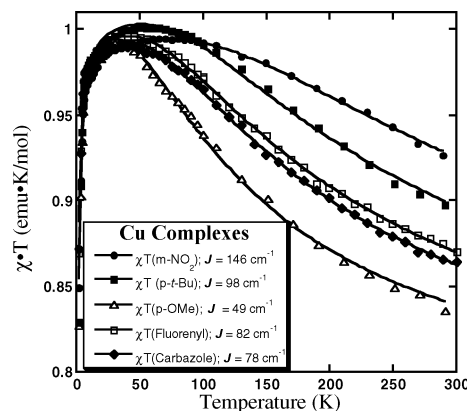
Table 1. Crystal Data and Structure Refinement for **7c**, **7e**, and **8f**

	7c	7e	8f
empirical formula	C ₅₅ H ₆₁ BMnN ₇ O ₄	C ₇₂ H ₈₄ BMnN ₈ O ₂	C ₅₉ H ₆₇ BCuN ₆ O ₃
fw	949.86	1159.22	982.56
temp (K)	150(2)	150(2)	148(2)
wavelength (Å)	0.71073	0.71073	0.71073
cryst syst	monoclinic	triclinic	monoclinic
space group	<i>P2₁/c</i>	<i>P1</i>	<i>P2₁/c</i>
unit cell dimensions	<i>a</i> = 19.4248(18) Å <i>b</i> = 12.5501(12) Å <i>c</i> = 21.946(2) Å α = 90° β = 106.989(4)° γ = 90°	<i>a</i> = 15.711(2) Å <i>b</i> = 15.731(2) Å <i>c</i> = 17.097(2) Å α = 67.949(5)° β = 64.536(5)° γ = 76.334(6)°	<i>a</i> = 12.5993(9) Å <i>b</i> = 15.8485(9) Å <i>c</i> = 26.5416(15) Å α = 90° β = 99.247(4)° γ = 90°
vol (Å ³)	5116.6(9)	3521.9(9)	5231.0(6)
Z	4	2	4
density _{calcd} (Mg/m ³)	1.233	1.093	1.248
abs coeff (mm ⁻¹)	0.310	0.234	0.47
<i>F</i> (000)	2008	1236	2086.45
cryst size (mm)	0.32 × 0.11 × 0.03	0.24 × 0.20 × 0.06	0.36 × 0.26 × 0.18
cryst color/shape	red-brown plate	brown plate	green prism
θ range	2.72–20.41	2.71–19.92	1.20–25.00
limiting indices	–20 < <i>h</i> < 19 –13 < <i>k</i> < 13 –23 < <i>l</i> < 23	–13 < <i>h</i> < 15 –14 < <i>k</i> < 15 –17 < <i>l</i> < 17	–14 < <i>h</i> < 14 0 < <i>k</i> < 18 0 < <i>l</i> < 31
reflns collected	41015	24031	9101
independent reflns	6692	7442	9100
refinement method	full-matrix least-squares on <i>F</i> ²	full-matrix least-squares on <i>F</i> ²	full-matrix least-squares on <i>F</i>
data/restraint/params	6692/0/621	7442/0/807	6383/–/899
GOF on <i>F</i> ²	1.002 (<i>F</i> ²)	0.960 (<i>F</i> ²)	1.32 (<i>F</i>)
final <i>R</i> ^a indices [<i>I</i> > 2 σ (<i>I</i>)]	<i>R</i> _{gt} = 0.0529 w <i>R</i> _{gt} = 0.1072 <i>R</i> = 0.1203 w <i>R</i> = 0.1339	<i>R</i> _{gt} = 0.0660 w <i>R</i> _{gt} = 0.1606 <i>R</i> = 0.1322 w <i>R</i> = 0.1870	<i>R</i> _{gt} = 0.040 w <i>R</i> _{gt} = 0.39 <i>R</i> = 0.40 w <i>R</i> = 0.39
<i>R</i> ^a indices (all data)			

^a For **7c** and **7e**: $w = 1/[\sigma^2(F_o^2) + (0.1056P)^2 + 0.0000P]$, where $P = (F_o^2 + 2F_c^2)/3$. For **8f**: $R_f = \sum(|F_o - F_c|)/\sum F_o$, $R_w = [\sum(w(F_o - F_c)^2)/\sum(F_o^2)]$, $GOF = [\sum(w(F_o - F_c)^2)/(\text{no. of reflns} - \text{no. of params})]$.

**Figure 2.** $\text{Tp}^{\text{Cum,Me}}\text{Mn}^{\text{II}}(\text{SQ-Ar})$ (**7a–7e**) χT vs *T* plots.

All of our Cu-SQ-Ar exchange coupling parameters are more weakly ferromagnetic than the corresponding *J* value reported by Pierpont and co-workers²⁷ ($J_{\text{Cu-SQ}} \geq +200 \text{ cm}^{-1}$) for $\text{Tp}^{\text{Cum,Me}}\text{Cu}(\text{DBSQ})$, where DBSQ = 3,5-di-*tert*-butylsemiquinone. The DBSQ ligand lacks the delocalizing aryl groups that our ligands have. Since the aryl groups of ligands **5** and **6** delocalize spin density and thereby decrease the spin density on the atoms of the SQ group, the observed weaker coupling in our Cu complexes compared to $\text{Tp}^{\text{Cum,Me}}\text{Cu}(\text{DBSQ})$ is consistent with a dominant ferromagnetic direct exchange contribution to $J_{\text{Cu-SQ}}$.

**Figure 3.** $\text{Tp}^{\text{Cum,Me}}\text{Cu}^{\text{II}}(\text{SQ-Ar})$ (**8a**, **8e**, and **8f–h**) χT vs *T* plots.

Conclusions

The changes observed in the magnitude of *J* for the Mn^{II}- and $\text{Tp}^{\text{Cum,Me}}\text{Cu}^{\text{II}}(\text{SQ-Ar})$ complexes in this work are indicative of a substituent effect, perhaps combined with a ligand conformation effect. The apparent lack of a straightforward correlation between the magnitude of *J* and various substituents for the Mn^{II} complexes is most likely a consequence of the multiple spin-exchange pathways possible.

The substituent effects observed for the $\text{Tp}^{\text{Cum,Me}}\text{Cu}^{\text{II}}(\text{SQ-Ar})$ complexes are encouraging and suggest likely design features for maximizing or modulating *J*. Undoubtedly, the fact that Cu^{II} has one dominant superexchange pathway with

Substituent Effects on Exchange Coupling

Table 2. $T_{\text{P}}^{\text{Cum,MeMn}^{\text{II}}(\text{SQ-Ar})}$ and $T_{\text{P}}^{\text{Cum,MeCu}^{\text{II}}(\text{SQ-Ar})}$
Variable-Temperature Magnetic Susceptibility Fit Parameters

	substituent	J (cm^{-1})	zJ' (cm^{-1})	g
7a	<i>m</i> -NO ₂	-68.7 ± 0.3	-0.19 ± 0.01	2.10 ± 0.01
7b	<i>m</i> -CN	-75.4 ± 1.2	-0.16 ± 0.01	2.09 ± 0.01
7c	<i>p</i> -NO ₂	-110.4 ± 2.3	-0.21 ± 0.01	2.15 ± 0.01
7d	<i>p</i> -CN	-82.2 ± 2.0	-0.27 ± 0.01	2.12 ± 0.01
7e	<i>p-t</i> -Bu	-120.0 ± 1.6	-0.16 ± 0.01	2.10 ± 0.01
8a	<i>m</i> -NO ₂	+146.2 ± 3.8	-0.28 ± 0.01	1.98 ± 0.01
8e	<i>p-t</i> -Bu	+97.9 ± 2.1	-0.34 ± 0.01	1.98 ± 0.01
8f	<i>p</i> -OCH ₃	+48.7 ± 0.7	-0.37 ± 0.01	1.99 ± 0.01
8g	fluorenyl	+81.5 ± 0.5	-0.13 ± 0.01	2.00 ± 0.01
8h	carbazole	+77.6 ± 0.6	-0.12 ± 0.02	1.99 ± 0.01

SQ-Ar (compared to Mn^{II}) will permit a more straightforward interpretation of the substituent effects. From our results, it appears that mesomeric substituents, Ar, will decrease the ferromagnetic contribution via direct exchange to J for LCu-(SQ-Ar), but in a series of SQ-Ar ligands, a more-withdrawing Ar will have a more ferromagnetic J .

In all cases, collection and analysis of additional X-ray data combined with electronic absorption spectroscopy will

be essential to fully resolve the complicated mechanisms of exchange coupling between paramagnetic transition metal ions and SQ ligands. Future work along these lines is planned.

Acknowledgment. The views expressed in this academic research paper are those of the authors and do not necessarily reflect the official policy or position of the U.S. Government, the Department of Defense, or any of its agencies. The authors would like to thank the NCSU Mass Spectrometry Facility for high-resolution MS analysis, the NCSU X-ray Facility, and the University of Michigan X-ray Facility for crystallography support. D.A.S. thanks the National Science Foundation (CHE-0345263) for support of this work.

Supporting Information Available: Synthetic details and X-ray crystallographic files in CIF format. This material is available free of charge via the Internet at <http://pubs.acs.org>.

IC061807G